Magnetic field induced formation of a stationary charge density wave in a conducting Möbius stripe

Sevak Demirchyan [1,2,3,4,*] and Alexey Kavokin [1,2,†]

[1] *School of Science, Westlake University, 18 Shilongshan Road, Hangzhou 310024, Zhejiang Province, China*
[2] *Institute of Natural Sciences, Westlake Institute for Advanced Study, 18 Shilongshan Road, Hangzhou 310024, Zhejiang Province, China*
[3] *Department of Physics and Applied Mathematics, Vladimir State University, Gorkii Street 87, Vladimir 600000, Russia*
[4] *Russian Quantum Center, Skolkovo IC, Bolshoy Bulvar 30, bld. 1, Moscow 121205, Russia*

(Received 24 February 2021; revised 27 May 2021; accepted 1 June 2021; published 11 June 2021)

Magnetic field induced edge currents propagate in opposite directions at opposite edges of a Hall bar. We consider a system that possesses just one edge: a Möbius stripe. We show that if the carrier mean free path is less than the width of the stripe, magnetic field induced edge currents vanish. Instead, a stationary charge density wave is formed. Its profile is governed by the interplay between the magnetic field dependence of the chemical potential and the screened Coulomb repulsion of charge carriers. This effect offers an experimental tool for studies of the electron density of states in two-dimensional crystal films.

DOI: 10.1103/PhysRevB.103.245416

I. INTRODUCTION

At equilibrium, an isolated nonsuperconducting solid state system subject to a stationary magnetic field cannot propagate conventional electric currents for a simple reason: The work of a stationary Lorentz force is always zero (see e.g., [1–3]). Still, nondissipative edge currents may propagate. Edge currents induced by a strong magnetic field in a metal or semiconductor crystal represent an electron transport effect that is unique from many points of view [4,5]. Edge currents are ballistic in their nature. They may be generated at zero applied voltage solely under an effect of the Lorentz force provided that the electron mean free path strongly exceeds its cyclotron orbit diameter [5]. In this regime, scattering of carriers plays no significant role, which is why edge currents are dissipationless and may propagate persistently. Furthermore, these currents are topologically protected, the value and the direction of each current is only dependent on the topology of the edge, temperature, and the magnitude of the applied magnetic field [6,7]. A great number of publications is devoted to the studies of edge currents in the quantum Hall regime, where they play a crucial role [4,8,9]. Recently, we have shown how persistent edge currents in a Corbino disk [7] may affect the macroscopic diamagnetic response of the system. In this context, as we show below, the topology of a Möbius stripe offers an interesting example of a system where edge currents cannot propagate in the stationary regime (excluding the limiting case of strictly no scattering). A Möbius stripe is a famous example of a self-connected surface that possesses just one edge. A quantum-mechanical description of electron transport on a Möbius ring and its comparison with conventional ring geometry was made in [10], the effects caused by the topology of the Möbius stripe were described for both metals [11] and graphene [12]. If a Möbius stripe is subject to an uniform stationary magnetic field, on its surface one can always draw a crossing line that is parallel to the field, and another crossing line that is perpendicular to the field. A convenient way to describe the edge of a Möbius stripe is by introducing an angular coordinate θ that spans the interval between 0 and 4π as one describes the full circle and comes back to the point of departure following the edge. The normal to the plane of the stripe projection of the external magnetic field H depends on θ as $H = H_0 \sin\theta/2$, where H_0 is the magnitude of the applied field. One can see in Fig. 1(a) that between $\theta = 0$ and $\theta = 4\pi$, H crosses 0 and changes its sign twice. Figure 1(b) shows schematically the trajectories of carriers that might contribute to the edge currents for different values and signs of H. We assume that for positive H the direction of cyclotron motion of the carriers is clockwise. One can see that the direction of the edge current changes at $\theta = 0$ and $\theta = 2\pi$. Currents flow from both sides towards one of these points and away from the other one. Obviously, in the stationary regime, the electric charge cannot accumulate continuously in the vicinity of zero field points. In the absence of scattering, the currents must jump between the edges of the stripe near $\theta = 0$ and $\theta = 2\pi$ points, so that the system would propagate two currents of the same magnitude simultaneously: one going clockwise and another one going anticlockwise. These currents cross each other when jumping between the edges of the stripe in the vicinity of zero magnetic field points [13]. In this, ballistic, regime, the coherence of propagating quasiparticles is never broken and interesting interference effects such as the analog of Aharonov-Bohm [14] effect may be observed. However, this regime is unlikely to be realised in macroscopic crystal structures at nonzero temperatures. Indeed, in macroscopic structures, the width of the stripe D must be expected to be much larger than the mean free path of propagating carriers. Hence, the current between opposite sides of the stripe must be dissipative rather than ballistic [15]. The propagation of dissipative currents would result in a permanent generation

*sevakdemirchyan@gmail.com
†a.kavokin@westlake.edu.cn

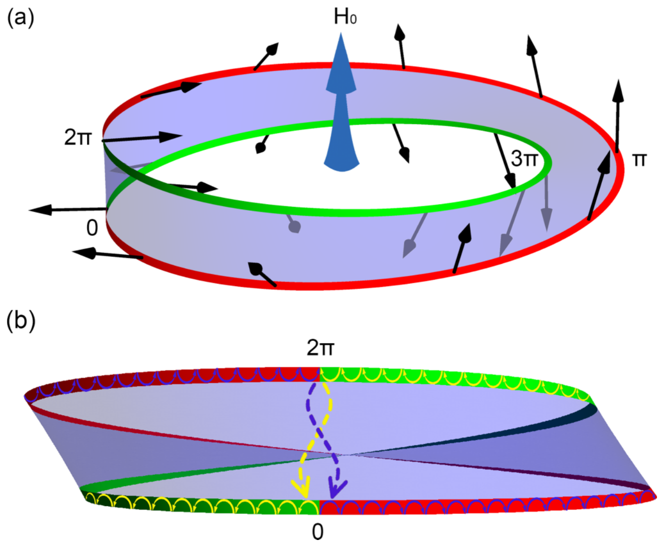

FIG. 1. (a) A conducting Möbius stripe subjected to a magnetic field. The red line along the edge corresponds to the area where the normal to the plane projection of the magnetic field is positive, the green line shows where it is negative. (b) The trajectories of cyclotron orbits of charge carriers for a section of the Möbius stripe near the points 0 and 2π.

of heat out of nowhere, that would be equivalent to the realization of a *perpetuum mobile*. Clearly, this is impossible. One should conclude that in a realistic Möbius stripe the circuit of edge currents is broken in the vicinity of $\theta = 0$ and $\theta = 2\pi$ points, so that no current can be flowing in the system. Still, this regime offers some beautiful physics that can be studied experimentally and theoretically. In this work, we present an analytical theory that describes the profile of a charge density wave (CDW) [16,17] that forms itself along the edge of a conducting Möbius stripe subjected to a strong spatially uniform magnetic field. We also consider the ballistic regime, where the CWD is not form, and edge currents in both directions do propagate.

II. CHARGE DENSITY WAVE

We shall describe the Coulomb repulsion of charge carriers with use of the standard screened Poisson equation written in form of a Klein-Gordon equation [18,19] that links the electron density δn_{3D} with the electrostatic potential ϕ:

$$\left(\frac{1}{R^2}\frac{d^2}{d\theta^2} - \lambda^2\right)\phi = \frac{e\delta n_{3D}}{\epsilon_0\epsilon}, \tag{1}$$

where R is a radius of the Möbius stripe, λ is the reverse screening length, ϵ is a dielectric constant. For simplicity, we write Eq. (1) in a one-dimensional form while it can be easily generalised to the two-dimensional case that would enable one to account for the decay of CDW as one moves away from the edge of the stripe.

Assuming that radius R of the Möbius stripe is much larger than any characteristic length in the system, we can neglect the first term in Eq. (1) and obtain a linear dependence of the electrostatic potential on the electron density:

$$\phi = -\frac{e}{\lambda^2\epsilon\epsilon_0}\delta n_{3D}. \tag{2}$$

In what follows we shall operate with the two-dimensional electron density defined as $n_{2D} = n_{3D}L$, where L is the thickness of the stripe. The variation of carrier concentration is defined as $\delta n_{2D} = n_{2D} - n_0$, where n_0 is the uniformly distributed electron density in the absence of the magnetic field. We shall follow the approach of [1] and [20] who postulate the constancy of the electrochemical potential at thermal equilibrium:

$$\mu - e\phi = \text{const}. \tag{3}$$

We shall also assume that the chemical potential is coordinate-dependent. Note that an alternative concept that defines the electrochemical potential locally and postulates the constancy of chemical potential at equilibrium would yield exactly the same result.

The concentration of carriers in a 2D-electron gas depends on the chemical potential, temperature, and magnetic field [21]:

$$n_{2D} = 2\frac{S(\mu)}{(2\pi\hbar)^2} + \frac{m\omega_c}{\pi^2\hbar} \times \arctan\frac{\sin 2\pi\left(\frac{S(\mu)}{2\pi\hbar e|H|} - \gamma\right)}{e^{\frac{2\pi kT_D}{\hbar\omega_c}} - \cos 2\pi\left(\frac{S(\mu)}{2\pi\hbar e|H|} - \gamma\right)}, \tag{4}$$

where $S(\mu)$ is the cross section of the Fermi surface, m is the electron effective mass, ω_c is the cyclotron frequency that is defined by the component of the magnetic field that is normal to the plane of the stripe, T_D is the Dingle temperature that describes the broadening of Landau levels [22], and γ is the topological parameter that allows to distinguish between carriers having a parabolic energy spectrum and Dirac fermions [23].

Equations (2)–(4) form a closed system that can be resolved for any specific value of θ. As a result, the stationary distribution $n(\theta)$ can be obtained that describes the CDW in a Möbius stripe. (We will omit the superscripts 2D from now on for simplicity.)

Substituting Eqs. (2) and (4) into Eq. (3) one can obtain an equation for the angle-dependent chemical potential:

$$\mu + \frac{e^2}{\lambda^2\epsilon\epsilon_0 L}\left[2\frac{S(\mu)}{(2\pi\hbar)^2} + \frac{m\omega_c}{\pi^2\hbar} \times \arctan\frac{\sin 2\pi\left(\frac{S(\mu)}{2\pi\hbar e|H|} - \gamma\right)}{e^{\frac{2\pi kT_D}{\hbar\omega_c}} - \cos 2\pi\left(\frac{S(\mu)}{2\pi\hbar e|H|} - \gamma\right)} - n_0\right] = C. \tag{5}$$

The value of the constant in the right part of Eq. (5) is defined by the normalization condition. The integrated variation of the electronic concentration along the entire edge of the Möbius stripe must be zero:

$$\int_0^{4\pi} \delta n_{2D} d\theta = 0. \tag{6}$$

As an example of a system sustaining a 2D-electron gas characterised by a parabolic dispersion, we consider an ultrathin metallic foil. We refer to a multitude of works reporting

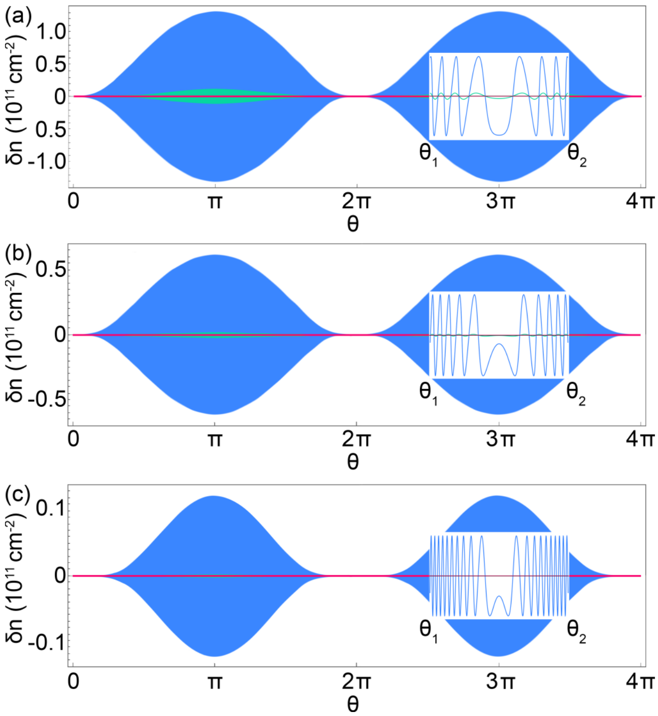

FIG. 2. Variation of the electron density at the edge of a metallic Möbius stripe as a function of the angular coordinate calculated at different values of the applied magnetic field: (a) $H_0 = 15$ T, (b) $H_0 = 10$ T, (c) $H_0 = 5$ T. Blue, green, and red lines correspond to the values of the Dingle temperature: $T_D = 2$ K, $T_D = 10$ K, and $T_D = 50$ K, respectively. The insets show on a larger scale the distribution of the electron density in the vicinity of the 3π point ($\theta_1 = 3\pi - \frac{\pi}{32}; \theta_2 = 3\pi + \frac{\pi}{32}$).

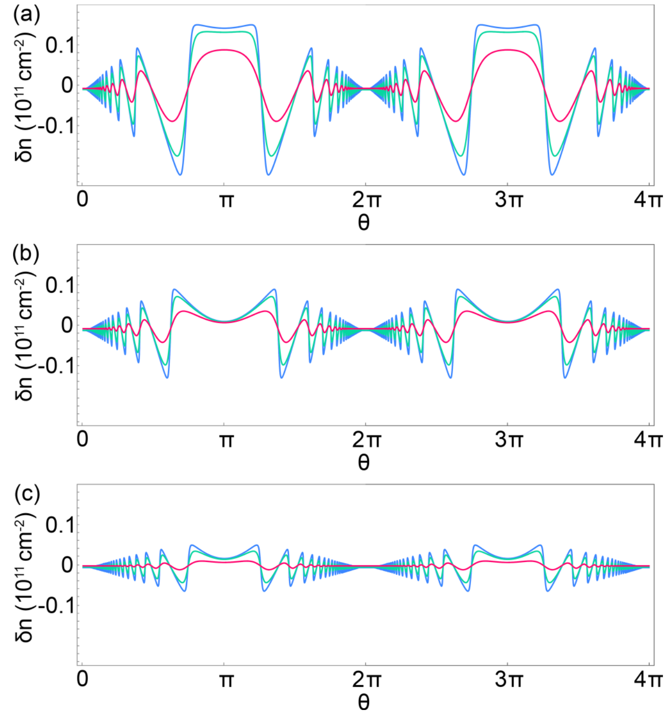

FIG. 3. Variation of the electron density at the edge of the graphene Möbius stripe as a function of the angular coordinate calculated at different values of the applied magnetic field: (a) $H_0 = 15$ T, (b) $H_0 = 10$ T, (c) $H_0 = 5$ T. Blue, green, and red lines correspond to the Dingle temperatures $T_D = 2$ K, $T_D = 10$ K, and $T_D = 50$ K, respectively.

fabrication of a micrometer scale metallic rings [24,25] and strongly believe that the fabrication of a metallic Möbius stripe is within the reach of modern technologies. We introduce the reverse screening length for normal carriers in the Thomas-Fermi approximation:

$$\lambda_{NC} = \frac{me^2}{2\pi\epsilon_0\epsilon\hbar^2}. \tag{7}$$

The Fermi surface cross-section writes [21]

$$S(\mu) = 2\pi m\mu. \tag{8}$$

The other parameters essential for the calculation are: $\omega_c = e|H|/m,\ \gamma = 1/2,\ L = 50$ nm, $m = m_0$, where m_0 is the free electron mass. We estimate for the static dielectric permittivity in metals as $\epsilon = 1$ [26]. Figure 2 shows the calculated profiles of CDW in a metallic Möbius stripe at different values of magnetic fields and Dingle temperatures. We took the Fermi energy of a two-dimensional electron gas in a metal to be 4.8 eV, which roughly corresponds to gold. One can see that the oscillations of the electron density become stronger at stronger magnetic fields. Also, one can see that the magnitude of oscillations decreases with the increase of the Dingle temperature, which characterizes the broadening of Landau levels. Sharp oscillation of the carrier density for $H_0 = 15$ T, $T_D = 2$ K, which are shown by the blue curve in the inset in Fig. 2(a) are almost washed out at the magnetic field $H_0 = 5$ T and Dingle temperature $T_D = 50$ K as shown by the red curve in the inset to Fig. 2(c). It is instructive to compare the profile of CDW calculated for carriers having a parabolic dispersion with the corresponding profile obtained for Dirac fermions characterized by a linear dispersion. We shall consider graphene, where charge carriers are characterized by the $\sim k^{1/2}$ Landau energy spectrum, with k being the Landau quantum number [27]. The reverse screening length for Dirac fermions in the Thomas-Fermi approximation is [28]

$$\lambda_{DF} = \frac{\mu e^2}{\pi\epsilon_0\epsilon\hbar^2 v^2}, \tag{9}$$

where v is the Fermi velocity. For Dirac fermions [21]

$$S(\mu) = \pi\frac{\mu^2}{v^2}. \tag{10}$$

The other parameters become $\omega_c = e|H|v^2/\mu,\ \gamma = 0,\ \epsilon = 6.9,\ L = 0.22$ nm, $v = 10^8$ cm/s [27,29].

The solutions of Eq. (5) in the case of a graphene Möbius stripe for various values of the magnetic field and Dingle temperatures are shown in Fig. 3. One can see that the variation of the electron density along the edge of the stripe is qualitatively similar to one obtained in the case of metal. However, the positively and negatively charge parts are redistributed in the real space. The difference in a shape of CDW for carriers with a parabolic dispersion and Dirac fermions is governed by the topological parameter γ that takes values 1/2 and 0 for the two types of carriers, respectively. We note

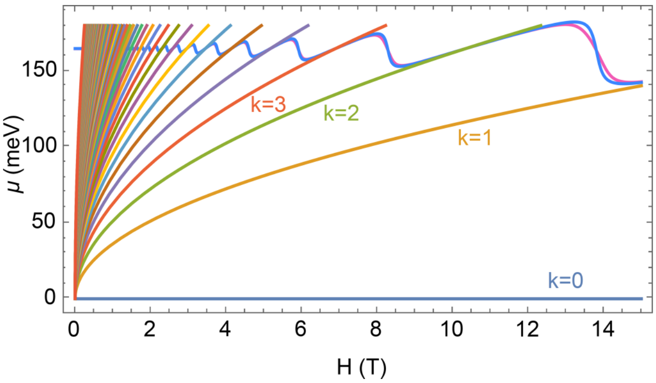

FIG. 4. The electronic chemical potential as a function of the normal-to-plane magnetic field calculated for a graphene Möbius stripe in the presence (red line), and in the absence (blue line) of the electron density redistribution caused by the CDW effect. Labeled lines show the energies of the corresponding Landau levels as functions of the magnetic field. $T_D = 10$ K is assumed.

that also the magnitude of the electron density oscillations in graphene is smaller than in metallic foil because of the lower Fermi energy.

To shed light on the mechanism of the CDW formation in the Möbius stripe, it is instructive to compare the angular dependencies of the chemical potential calculated accounting for and neglecting the formation of the CDW. In the latter case we need to assume a constant charge density along the edge of the stripe. In order to perform this analysis, we invert Eq. (4) following [27,30] and obtain

$$S(\mu) = 2\hbar^2\pi^2 n - 2\hbar e|H| \times \arctan\frac{\sin 2\pi\left(\frac{\pi\hbar n}{e|H|} - \gamma\right)}{e^{\frac{2\pi k T_D}{\hbar\omega_c}} + \cos 2\pi\left(\frac{\pi\hbar n}{e|H|} - \gamma\right)}. \tag{11}$$

Using Eqs. (10) and (11) one can calculate the chemical potential for a graphene for a uniformly distributed electron density that is taken to be $n_0 = 10^{12}$ cm^{-2}. Figure 4 shows the chemical potential calculated as a function of the normal-to-plane projection of the magnetic field in the presence and in the absence of the charge density redistribution (red and blue curves, respectively).

One can see that the oscillations of the chemical potential are dumped by the redistribution of the electron charge. Clearly, the system tends to reduce the spatial inhomogeneity of the chemical potential. The price to pay for smoothing of the chemical potential profile is the induced inhomogeneity of the electron density, i.e., the CDW effect.

III. EDGE CURRENTS

Here we consider the ballistic limit where carriers can "jump" from one to another side of the stripe as Fig. 1(b) shows. In this regime, the Möbius stripe represents a two-dimensional Chern insulator [13]. The net contribution to the current from a single electron moving along the edge of the stripe on a ballistic trajectory is

$$\vec{i} = -\frac{e^2}{mc}\frac{\vec{A}}{2\pi R}. \tag{12}$$

The circulation of the current can be evaluated with use of the Stokes theorem,

$$\oint_L \vec{i}d\vec{r} = -\frac{e^2}{mc}\frac{1}{2\pi R}\oint_L \vec{A}d\vec{r} = -\frac{e^2}{mc}\frac{1}{2\pi R}\int \vec{H}d\vec{S} = -\frac{e^2}{mc}\frac{\Phi}{2\pi R}\vec{e}_n, \tag{13}$$

where R is radius of the Möbius stripe, which is assumed to be much larger than any characteristic length in the system. Φ is the magnetic flux through the surface limited by a circle formed by the central line of the Möbius stripe, $\vec{e}_n$ is a unit vector oriented along the axis of the stripe. In order to obtain the full current we need to estimate the total number of electrons moving over ballistic trajectories and able to accomplish a full round:

$$\vec{I} = \vec{i}N_e. \tag{14}$$

We assume that in the point where the magnetic field is perpendicular to the stripe Landau levels $n_L = 0, 1, ..., p-1$ are fully occupied accommodating $\tilde{N}$ electrons in total and the level p is partially occupied with $\lambda\tilde{N}$ electrons, where $0 \leqslant \lambda < 1$. One can express

$$N = \nu\tilde{N}, \tag{15}$$

where $\nu = p + \lambda$ is the filling factor, which is connected with the magnetic field magnitude as

$$\nu = \frac{n\phi_0}{H}, \tag{16}$$

where $n = N/S$ is the number of electrons per unit area and ϕ_0 is the flux quantum and in the case of spin degeneracy $\phi_0 = hc/2e$.

At each Landau level only those electrons that are separated from the edge by a distance that does not exceed the corresponding cyclotron radius:

$$r_{n_L} = \sqrt{\frac{(2n_L+1)\hbar c}{eH}} \tag{17}$$

can contribute to the current. In order to find the total number of electrons contributing to the edge currents, we multiply the two-dimensional electron density at each Landau level by the area occupied by electrons, which can contribute to the current. Next, we sum up the contribution of all filled levels and take into account the partially filled highest Landau level:

$$N_e = \sum_{n_L=0}^{p-1}\frac{n}{\nu}r_{n_L}2\pi R + \lambda\frac{n}{\nu}r_p 2\pi R. \tag{18}$$

Combining Eqs. (13) and (18) we obtain the identical clockwise and anticlockwise currents as functions of the magnetic field, see Fig. 5. It is important to note that, in contrast to the Corbino disk, in a Möbius stripe the magnitudes of clockwise and anticlockwise edge currents are always equal.

IV. CONCLUSIONS

We have shown that a one-dimensional stationary CDW may be formed along the edge of a conducting Möbius stripe in the presence of a strong magnetic field. CDW results

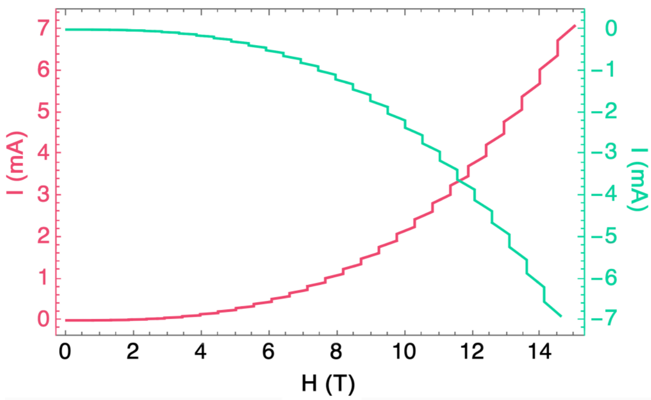

FIG. 5. The ballistic limit: clockwise and anticlockwise edge currents in a Möbius stripe are shown by green and red lines, respectively. No CDW is formed. We have used the parameters of a metallic foil $n = 0.2 \times 10^{16}$ cm^{-2}, $R = 5\ \mu$m.

from the electron density redistribution in real space that is governed by the interplay between the chemical potential dependence on the normal-to-plane projection of the magnetic field and the screened Coulomb repulsion of carriers. The predicted charge density variation is macroscopic and it may be significant at low temperatures. The electron density of states in a material that forms the stripe can be restored from the experimentally measured profile of the electron density distribution. At extremely low temperatures, in pure crystalline samples, a ballistic regime can be recovered where the electron mean free path exceeds the width of the stripe. In this regime, the CDW along the edge of the stripe is suppressed. Instead, nondissipative edge currents start flowing. Clockwise and anticlockwise edge currents in a Möbius stripe are exactly equal to each other. The topology of a Möbius stripe offers a powerful tool for studies of one-dimensional fermionic systems.

ACKNOWLEDGMENTS

The work is supported by the Westlake University, Project No. 041020100118 and Program No. 2018R01002 funded by the Leading Innovative and Entrepreneur Team Introduction Program of Zhejiang Province. The support from RFBR Grant 21-52-10005, from the Grant of the President of the Russian Federation for state support of young Russian scientists No. MK-5318.2021.1.2 is also acknowledged.

[1] A. A. Abrikosov, *Fundamentals of the Theory of Metals* (Dover Publications, New York, 2017).
[2] J. D. Jackson, *Classical Electrodynamics* (Wiley, New York, 1999).
[3] L. D. Landau, E. M. Lifshitz, and L. P. Pitaevskii, *Electrodynamics of Continuous Media*, 2nd ed. (Elsevier, Amsterdam, 2013).
[4] B. I. Halperin, Quantized Hall conductance, current-carrying edge states, and the existence of extended states in a two-dimensional disordered potential, Phys. Rev. B **25**, 2185 (1982).
[5] M. E. Cage, Current distributions in quantum Hall effect devices, J. Res. Natl. Inst. Stand. Technol. **102**, 677 (1997).
[6] C. L. Kane and M. P. A. Fisher, Edge-state transport, *Perspectives in Quantum Hall Effects* (Wiley-VCH Verlag GmbH, New York, 2007), pp. 109–159.
[7] A. V. Kavokin, B. L. Altshuler, S. G. Sharapov, P. S. Grigoryev, and A. A. Varlamov, The Nernst effect in Corbino geometry, Proc. Natl. Acad. Sci. USA **117**, 2846 (2020).
[8] M. Büttiker, Absence of backscattering in the quantum Hall effect in multiprobe conductors, Phys. Rev. B **38**, 9375 (1988).
[9] C. Altimiras, H. le Sueur, U. Gennser, A. Cavanna, D. Mailly, and F. Pierre, Non-equilibrium edge-channel spectroscopy in the integer quantum Hall regime, Nat. Phys. **6**, 34 (2010).
[10] Z. Li and L. R. Ram-Mohan, The Aharonov-Bohm effect with a twist: Electron transport through finite-width Möbius rings, J. Appl. Phys. **114**, 164322 (2013).
[11] Y. Yin, S. Li, V. Engemaier, E. Saei Ghareh Naz, S. Giudicatti, L. Ma, and O. G. Schmidt, Topology induced anomalous plasmon modes in metallic Möbius nanorings, Laser Photonics Rev. **11**, 1600219 (2017).
[12] K. Flouris, M. M. Jimenez, and H. J. Herrmann, Quantum spin-Hall effect on Möbius graphene ribbon, arXiv:1902.03892.
[13] L.-T. Huang and D. H. Lee, Topological Insulators on a Mobius Strip, Phys. Rev. B **84**, 193106 (2011).
[14] Y. Aharonov and D. Bohm, Significance of Electromagnetic Potentials in the Quantum Theory, Phys. Rev. **115**, 485 (1959).
[15] S. Olszewski, Quantum Aspects of the Joule-Lenz Law, J. Mod. Phys. **7**, 162 (2016).
[16] H. Fukuyama, P. M. Platzman, and P. W. Anderson, Two-dimensional electron gas in a strong magnetic field, Phys. Rev. B **19**, 5211 (1979).
[17] G. Grüner, The dynamics of charge-density waves, Rev. Mod. Phys. **60**, 1129 (1988).
[18] O. B. Klein, Quantentheorie und fünfdimensionale Relativitätstheorie, Z. Phys. **37**, 895 (1926).
[19] W. Gordon, Der comptoneffekt nach der schrödingerschen theorie, Z. Phys. **40**, 117 (1926).
[20] O. Madelung, *Introduction to Solid-State Theory* (Springer Science & Business Media, New York, 2012), Vol. 2.
[21] I. A. Luk'yanchuk, A. A. Varlamov, and A. V. Kavokin, Giant Nernst-Ettingshausen Oscillations in Semiclassically Strong Magnetic Fields, Phys. Rev. Lett. **107**, 016601 (2011).
[22] R. B. Dingle, Some magnetic properties of metals I. General introduction, and properties of large systems of electrons, Proc. Roy. Soc. London A **211**, 500 (1952).
[23] G. Mikitik and Y. Sharlai, Manifestation of Berry's Phase in Metal Physics, Phys. Rev. Lett. **82**, 2147 (1999).
[24] H. Bluhm, N. C. Koshnick, J. A. Bert, M. E. Huber, and K. A. Moler, Persistent Currents in Normal Metal Rings, Phys. Rev. Lett. **102**, 136802 (2009).
[25] A. C. Bleszynski-Jayich, W. E. Shanks, B. Peaudecerf, E. Ginossar, F. von Oppen, L. Glazman, and J. G. E. Harris,

Persistent currents in normal metal rings, Science **326**, 272 (2009).

[26] P. Lorrain and D. R. Corson, *Electromagnetic Fields and Waves* (W. H. Freeman, New York, 1970).

[27] I. A. Luk'yanchuk and Y. Kopelevich, Phase Analysis of Quantum Oscillations in Graphite, Phys. Rev. Lett. **93**, 166402 (2004).

[28] M. Jablan, M. Soljačić, and H. Buljan, Effects of screening on the optical absorption in graphene and in metallic monolayers, Phys. Rev. B **89**, 085415 (2014).

[29] J. Fang, W. Vandenberghe, and M. Fischetti, Microscopic dielectric permittivities of graphene nanoribbons and graphene, Phys. Rev. B **94**, 045318 (2016).

[30] T. Champel and V. Mineev, de Haas-van Alphen effect in two- and quasi-two-dimensional metals and superconductors, Philos. Mag. B **81**, 55 (2001).